10.3 THE RESPONSE OF SIMULATED NOCTURNAL CONVECTIVE SYSTEMS TO A LOW-LEVEL JET

Adam J. French* and Matthew D. Parker
North Carolina State University, Raleigh, North Carolina

1. INTRODUCTION

Warm season precipitation has long been observed to exhibit a nocturnal maximum over the central United States, attributed to a preponderance of nighttime thunderstorms and mesoscale convective systems (MCSs) that cross the region (e.g. Wallace 1975; Maddox 1980). Recent work by Parker (2008) (hereafter P08) has elucidated some of the dynamical processes at work within these nocturnal systems using idealized numerical simulations. In the interest of isolating these fundamental dynamics, these simulations utilized a simple, 2-D linear wind profile representative of an environment favoring strong MCSs. This, however, neglected a common feature found in nocturnal MCS environments: the nocturnal low-level jet (LLJ, e.g Maddox 1983; Cotton et al. 1989). In light of this, the present work looks to build upon the results of P08 to include the effects of a simulated nocturnal LLJ on elevated convection.

2. BACKGROUND

The LLJ has a long-standing association with warm-season precipitation in the central United States, particularly thunderstorms. The LLJ is recognized as a source of unstable air for convective storm development, largely through the advection of warm, moist air from the Gulf of Mexico into regions where storms develop (Maddox 1983; Cotton et al. 1989). These effects can be especially significant for nocturnal convection or storms that form and the cool side of frontal boundaries, as this LLJ-supplied high-θ_e air tends to be elevated. This provides a source of unstable air upon which storms can be sustained despite a stable boundary layer (e.g., Trier et al. 2006).

In addition to helping to prime the convective environment, the LLJ can be a significant forcing mechanism for long-lived convective systems, especially when the jet intersects a frontal boundary (e.g., Augustine and Caracena 1994). As the jet intersects the frontal boundary, convergence and frontogenetic forcing are enhanced, providing a lifting mechanism for storms (Trier and Parsons 1993; Trier et al. 2006; Tuttle and Davis 2006). As a forcing mechanism, the intensity of the jet has as a significant effect on storm intensity, with stronger jets being associated with heavier rainfall (Arritt et al. 1997; Tuttle and Davis 2006).

Missing from this collection of previous work is a discussion about how the development of the nocturnal jet may effect pre-existing convection, i.e. storms that have formed during the afternoon and continue into the overnight hours as the boundary layer stabilizes and the LLJ develops. Possible effects in this realm include changes in the vertical wind shear profile and modulations of the storm-relative inflow. Rotunno et al. (1988) developed a theory for squall line intensity and longevity based on a balance between the low-level shear and cold pool strength. As such, understanding the effect that the LLJ has on vertical shear could be important to better understanding the evolution of nocturnal convective systems. Additionally, Gale et al. (2002) suggested that a key determinant of nocturnal MCS dissipation is the strength of the elevated storm relative inflow (ESRI), with a decrease in this inflow leading to storm dissipation. Given the the LLJ tends to reside in or around the layer of ESRI, it may play a significant role in modulating the strength of this inflow. The present works looks to examine these effects using idealized numerical simulations.

3. METHODS

This work utilized 3D idealized numerical model simulations using version 1.10 of the Bryan cloud model (CM1) described by Bryan and Fritsch (2002). These simulations followed the setup described in P08, and the reader is referred to that publication for the specific details of the model configuration.

In order to study the effects of a low-level jet on

**Corresponding author address:* Adam J. French, Department of Marine, Earth, & Atmospheric Sciences, North Carolina State University, Campus Box 8208, Raleigh, NC 27695–8208. E-mail: ajfrench@ncsu.edu

nocturnal convective systems, it was of interest to include a low-level stable layer to represent the nocturnal environment. This was handled using the method of P08. A surface-based MCS was initiated using a warm (+ 2 K) line thermal, and allowed to mature through 3 hours. At this point a nocturnal stable layer was gradually introduced to the model by applying a cooling rate to the lowest 1 km of the simulated environment for the duration of the simulation. The resultant evolution simulates the transition from afternoon, surface-based convection to a nocturnal, elevated MCS akin to the "deep-unlim" simulation of P08.

The other necessary component for this study was the gradual addition of a jet structure to the low-levels of our simulation. Based on the results of past climatological studies, we chose to use a jet that was 5 ms^{-1} stronger than the background winds, approximately 1 km deep, with the level of maximum winds located just above the top of the nocturnal stable layer (e.g Bonner 1968; Mitchell et al. 1995; Whiteman et al. 1997). This jet was added to the wind profile in concert with the low-level cooling, gradually increasing to its maximum intensity by 8 hours into the simulation. This too was based on observations, as in nature the LLJ intensifies throughout the evening, reaching its maximum intensity around 0200 local time (e.g. Whiteman et al. 1997). This results in the perturbation wind profile shown in Fig. 1 by 8 hours into the simulation. It should be noted that while several climatologies (e.g. Bonner 1968; Whiteman et al. 1997) place the LLJ maximum winds at approximately 500 m, we chose to center the jet between 1 and 1.5 km as this was just above the simulated nocturnal stable layer, which is where the jet is typically observed. Sensitivity tests run to test different jet heights showed little effect on the simulated storm, so we chose 1 km in order to comply with the observed behavior of the jet being located just above the stable layer.

For the battery of simulations presented herein, the strength of the jet is held constant at 5 ms^{-1}stronger than the background winds, however the direction of the jet is varied. Three different jet directions are examined, relative to the simulated MCS: Front-to-rear (FTR), rear-to-front (RTF), and parallel (PAR) (Fig. 2). The varied configurations allow us to examine the effect that the direction of the jet has on both the vertical wind shear profile, as well as storm-relative inflow. In addition, we ran a control (CTL) simulation that did not include the LLJ, which is identical to the "deep-unlim" simulation of P08.

4. RESULTS

4.1 Overview

An examination of the CTL, FTR, RTF, and PAR simulations shows a fairly similar evolution through 8 hours of simulation. In each case, an initially surface-based MCS develops and evolves into an elevated MCS in a similar fashion to what was observed by P08. Throughout this period, comparisons of simulated radar reflectivity suggest that the MCSs in each simulation are fairly comparable in terms of size, intensity, and storm motion (not shown, the reader is referred to P'08 for a detailed analysis of the CTL simulation evolution). This similarity is maintained between the CTL and PAR simulations for the duration of the simulations, but not for the RTF and FTR simulations. After 8 hours (once the LLJ has reached its full intensity) the simulated MCSs in the FTR and RTF cases begin to diverge from the CTL and PAR simulations. Plan view plots of simulated radar reflectivity illustrate that by the end of the simulation (10 hours) the RTF case weakens considerably compared to the CTL simulation, while the FTR case is maintained at a similar or slightly stronger intensity (Fig. 3). It is also evident, from this analysis that the system speeds in the three simulations diverge during this period, with the RTF simulation exhibiting a faster forward motion compared to the CTL, and while the FTR is slower.

Plots of total upward mass flux (tmfu), total condensate (tcond), and total rainfall (train) (Fig. 4a, b, c) further illustrate the differences in storm intensity, as the FTR simulation features the strongest tmfu, tcond, and train from approximately 5 hours onward. This would suggest that the addition of the FTR jet enhances storm intensity and prolongs storm lifetime, as the MCS in the FTR simulation maintained a stronger intensity through the end of the 10 hour simulation (Fig. 3). That the PAR MCS exhibits behavior very similar to CTL MCS suggests that the LLJ has the most significant effect in the line-perpendicular direction. As a result, we focus our attention on the RTF and FTR simulations for the the remainder of this paper.

While the aforementioned analysis, primarily in terms of precipitation output, suggests that the FTR simulation generates a stronger storm, an analysis of maximum updraft speed (wmax) suggests otherwise. After approximately 8 hours (again, once the jet has reached maximum intensity) the RTF simulation features a stronger maximum updraft by approximately 5 ms^{-1} compared to the FTR simulation (Fig. 4d). This presents a slight conundrum in terms of evaluating storm intensity, as two common metrics, precipitation output and vertical velocity, provide differing answers as to which simulation produces a stronger storm. In order to further evaluate this dichotomy, we next analyze the processes at work in these simulations.

4.2 RKW Analysis

Rotunno et al. (1988) (hereafter RKW) presented a theory for long-lived squall lines that focuses on a balance between the strength of the horizontal vorticity generated by system's cold pool (c) and by the low-level environmental wind shear (Δu). In the "optimal" case, ($c/\Delta u \sim 1$) the vorticity generated by the cold pool is equal in magnitude and opposite in sign to that generated by the vertical shear. The result is a horizontal vorticity balance that produces a vertically oriented updraft, favoring deep lifting that readily transports parcels to their level of free convection (LFC) and thus sustains the convective system.

A wide range of updraft orientations were observed for the simulated cases in this study. Fig. 5 illustrates that the updraft in the CTL simulation is clearly sub-optimal, featuring a rearward tilt, and the FTR simulation is even less optimal. However, the RTF simulation features a considerably more erect updraft suggesting that it is more nearly optimal in the RKW sense. Given that the CTL run was sub-optimal to begin with, and that c is comparable between the runs, the more erect updraft featured in the RTF simulation is likely due to to an increase in vertical shear resulting from the addition of the LLJ.

In both the RTF and FTR cases, the vertical shear has increased below the level of maximum wind in the jet (Fig. 6). This owes to the prescribed shape of the jet, featuring a rapid increase in wind below the jet max, with a more gradual decrease above. However, the sign of ω_y is important, as it needs to oppose the ω_y generated by the bore (for the optimal case). The RTF case features enhanced ω_y of the appropriate sign (Fig. 6) to create a more RKW-optimal situation and to favor the erect updraft observed in Fig. 5. In the FTR case, the below-jet ω_y is of the same sign as that generated by the bore, suggesting sub-optimal conditions, which would explain the extreme rearward tilt of the updraft seen in Fig. 5. A layer of enhanced positive vorticity is present in the FTR simulation above the LLJ, centered at approximately 2100 m (Fig. 6). However, there is no CAPE present in this layer, and it is above the primary region of storm inflow, which suggests that these parcels are likely not playing a significant role in the maintenance of the simulated MCS.

Thus the addition of the LLJ does have a significant effect on storm structure and updraft strength. The RTF jet causes an increase in the shear that opposes the bore, with an associated increasingly vertical orientation of the updraft, as RKW theory would suggest. This accounts for the increased wmax seen in the RTF case. However, it does not explain why the FTR case has the larger precipitation output. To investigate this we analyze how the LLJ effects the storm relative inflow.

4.3 Storm Relative Inflow

In the case of elevated convection, the key to storm longevity is an elevated source of high-θ_e air that provides the inflow to sustain the storm (the ESRI discussed by Gale et al. 2002). A significant feature of the LLJ is that it tends to be located just above the top of a near-surface stable layer, within this layer of high-θ_e air. By altering the wind field within this zone of unstable air, the LLJ can have a significant effect on the ESRI that sustains an MCS (Gale et al. 2002). This was very evident in the case at hand, as the simulations including the RTF jet experienced a decrease in ESRI (represented by the storm relative mass flux in Fig. **7**b), while the simulations with the FTR jet featured an increase (Fig. **7**a).

These variations in ESRI ultimately correspond to differences in precipitation output. As warm, moist air parcels are fluxed into the storm they ascend through the the updraft region. More air being fluxed into the storm results in more parcels being lifted, more condensation taking place per unit time, and greater hydrometeor production. This increase in hydrometeor production ultimately results in an increase in precipitation output, as seen in the FTR simulation (i.e. Fig. 4b, c). The opposite can be observed within the RTF simulation, wherein decreased mass flux leads to fewer parcels being ingested into the storm and lifted, decreased hydrometeor production, and ultimately a decrease in precipitation.

Since the magnitude of the storm-relative winds are governed by the background wind profile as well as the storm motion, it is of interest to determine if the changes in ESRI were attributable to the addition of the LLJ alone, or due to variations in storm motion. From Fig. 8 it is clear that while the addition of the LLJ caused some change in the storm motion, these changes were generally small, with the RTF being about 1 ms^{-1} faster than the CTL and the FTR being about 1 ms^{-1} slower. These changes are trivial in comparison to the 5 ms^{-1} magnitude of the imposed LLJ. Additionally, since the RTF jet works to accelerate storm motion, if the changes in ESRI were due merely to differences in storm motion, then the ESRI would increase in the RTF case, which does not happen. Thus the changes in ESRI are likely due to the addition of the LLJ to the background wind profile, with the direction of the jet (toward or away from the system) playing a significant role in whether the ESRI is increased or decreased.

5. DISCUSSION

Based on the results discussed above, it is evident that the LLJ effects both the updraft tilt and the storm relative inflow. It is the latter of these that has the strongest effect on the intensity of the MCS. This makes sense, as at the most basic level it is the supply of high-θ_e air that is of primary importance to storm sustenance. Once this supply is cut off, or reduced as in the RTF case, the storm will weaken and dissipate. If this occurs, the tilt of the updraft becomes academic, as there are few/no parcels to be lifted by the updraft to sustain the storm. Thus the LLJ has the most significant effect on storm precipitation output by modulating the amount of mass that is ingested by the storm and subsequently condensed into precipitation.

This is not to discount the importance of updraft tilt when it comes to lifting parcels to their LFCs, as even the strongest storm-relative inflow will be of little consequence if cannot be sufficiently lifted. However, in the case at hand the depth of the bore lifting is sufficient for parcels to reach their LFCs via isentropic ascent (Fig. 9). The LFC for elevated parcels in this case is approximately 2 km, and the bore extends up to 2.5 km. As a result, in this case, storm precipitation output is governed by the amount of mass being fluxed into the storm by the storm-relative inflow, and the tilt of the updraft is of little importance.

6. CONCLUSIONS

Idealized numerical simulations were used to investigate the effects of a simulated nocturnal low-level jet on an elevated, nocturnal MCS. These simulations demonstrated two primary results. First, the addition of the LLJ has a dramatic effect on the low-level vertical wind shear within the jet layer, with the direction of the jet governing whether the shear is increased or decreased in this layer. This change in shear can in turn have a notable effect on the tilt of the storm's updraft, as discussed by RKW.

Second, the addition of the low-level jet works to modulate the storm relative inflow, again with the direction of the jet governing whether the inflow increases or decreases. This change in storm-relative inflow appeared to have the most significant effect on storm intensity in terms of precipitation output. The FTR (RTF) jet resulted in increased (decreased) storm relative inflow, and an associated increase (decrease) in intensity. Thus the presence of the LLJ appears to play an important role in modulating storm intensity beyond merely priming the environment for convection or providing a forcing mechanism as outlined in prior studies.

These results also suggest that, provided that parcels can readily reach their LFCs, the tilt of the updraft determined by the cold pool/shear balance theory presented by RKW, is of secondary importance to the strength of the storm-relative inflow when it comes to determining storm intensity. This is not to say that the tilt of the updraft is not important in cases wherein parcels need to be displaced to a greater altitude to reach their LFC, but rather that in the case at hand it was of little importance. This finding may help explain observed cases of intense squall lines such as derechos that are far from optimal in terms of cold pool/shear balance, yet persist as intense storms for long durations. Since these types of MCSs tend to feature deep cold pools and rapid forward motion, the depth of the cold pool may be sufficient to displace parcels to their LFC while the rapid forward motion would tend to enhance storm-relative inflow in a similar manner to the FTR jet presented herein, leading to long-lived intense squall lines.

7. FUTURE WORK

In order to fully examine the role of horizontal mass fluxes, several additional experiments have been proposed. First, the experiments presented herein focused solely on changing the direction of the LLJ, while holding the jet speed constant. It is of interest to examine any effects that a change in LLJ speed has on storm intensity and longevity. This may be particularly significant in modulating horizontal mass flux, as a faster jet would likely amplify the effects seen in the present study. Additionally, along the lines of the work of Corfidi et al. (1996) and Corfidi (2003) it would be of interest to run some completely 3D simulations (i.e. with a convective line that does not span the entire model domain) using the parallel jet described herein, or perhaps a jet oriented at an angle to the line. Previous work has demonstrated that surface-based MCS motion is strongly related to low-level shear and inflow, and it would be useful to determine if these parameters govern elevated MCS motion as well.

Acknowledgments

The authors would like to thank Ben Baranowski, as well as the other members of the Convective Storms Group at North Carolina State University for their helpful discussions and technical assistance during the course of this project. This work was funded by NSF grant ATM0552154.

References

Arritt, R. W., T. D. Rink, M. Segal, D. P. Todey, and C. A. Clark, 1997: The great plains low-level jet during the warm season of 1993. *Mon. Wea. Rev.*, **125**, 2176–2192.

Augustine, J. A. and F. Caracena, 1994: Lower tropospheric precursors to nocturnal mcs development over the central united states. *Wea. Forecasting*, **9**, 116–135.

Bonner, W. D., 1968: Climatology of the low level jet. *Mon. Wea. Rev.*, **96**, 833–850.

Bryan, G. H. and M. J. Fritsch, 2002: A benchmark simulation for moist nonhydrostatic numerical models. *Mon. Wea. Rev.*, **128**, 3941–3961.

Corfidi, S. F., 2003: Cold pools and mcs propagation: Forecasting the motion of downwind-developing mcss. *Wea. Forecasting*, **18**, 997–1017.

Corfidi, S. F., J. H. Merritt, and J. M. Fritsch, 1996: Predicting the movement of mesoscale convective complexes. *Wea. Forecasting*, **11**, 41–46.

Cotton, W. R., M. S. Lin, R. L. McAnelly, and C. J. Tremback, 1989: A composite model of mesoscale convective complexes. *Mon. Wea. Rev.*, **117**, 765–783.

Gale, J. J., W. A. Gallus, Jr, and K. A. Jungbluth, 2002: Toward improved prediction of mesoscale convective system dissipation. *Wea. Forecasting*, **17**, 856–872.

Maddox, R. A., 1980: Mesoscale convective complexes. *Bull. Amer. Meteor. Soc.*, **61**, 1374–1387.

———, 1983: Large scale meteorological conditions associated with midlatitude mesoscale convective complexes. *Mon. Wea. Rev.*, **111**, 1475–1493.

Mitchell, M. J., R. W. Arritt, and K. Labas, 1995: A climatology of the warm season great plains low-level jet using wind profiler observations. *Wea. Forecasting*, **10**, 576–591.

Parker, M. D., 2008: Respsons of simulated convective squall lines to low-level cooling. *J. Atmos. Sci.*, **65**, 1323–1341.

Rotunno, R., J. B. Klemp, and M. L. Weisman, 1988: A theory for strong, long–lived squall lines. *J. Atmos. Sci.*, **45**, 463–485.

Trier, S. B., C. A. Davis, D. A. Ahijevych, M. L. Weisman, and G. H. Bryan, 2006: Mechanisms supporting long-lived episodes of propagating nocturnal convection within a 7-day wrf model simulation. *J. Atmos. Sci.*, **63**, 2437–2461.

Trier, S. B. and D. B. Parsons, 1993: Evolution of environmental conditions preceding the development of a nocturnal mesoscale convective complex. *Mon. Wea. Rev.*, **121**, 1078–1098.

Tuttle, J. D. and C. A. Davis, 2006: Corridors of warm season precipitation in the central united states. *Mon. Wea. Rev.*, **134**, 2297–2317.

Wallace, J. M., 1975: Diurnal variations in precipitation and thunderstorm frequency over the conterminous united states. *Mon. Wea. Rev.*, **103**, 406–419.

Whiteman, C. D., X. Bian, and S. Zhong, 1997: Low-level jet climatology from enhanced rawinsonde observations at a site in the southern great plains. *J. Appl. Meteor.*, **36**, 1363–1376.

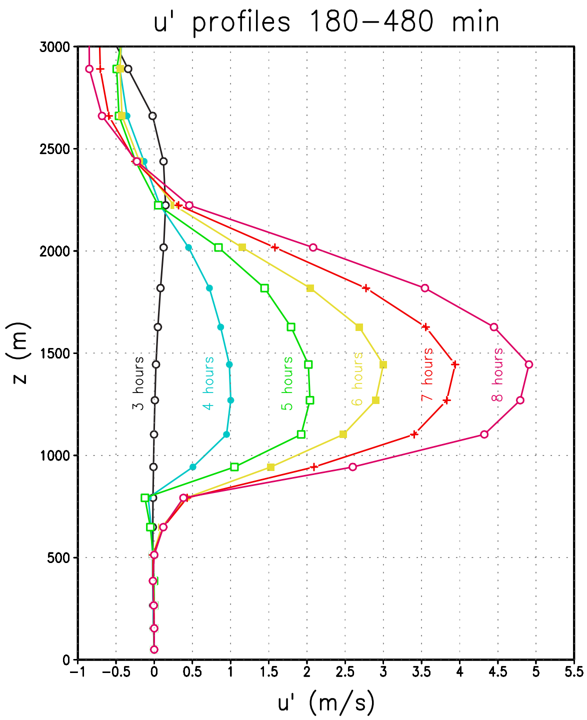

Figure 1: Time-series of hourly vertical perturbation u-wind profiles illustrating the development of the simulated LLJ. This plot is for the rear-to-front (RTF) case, however the front-to-rear (FTR) case has an identical shape, but of opposite sign.

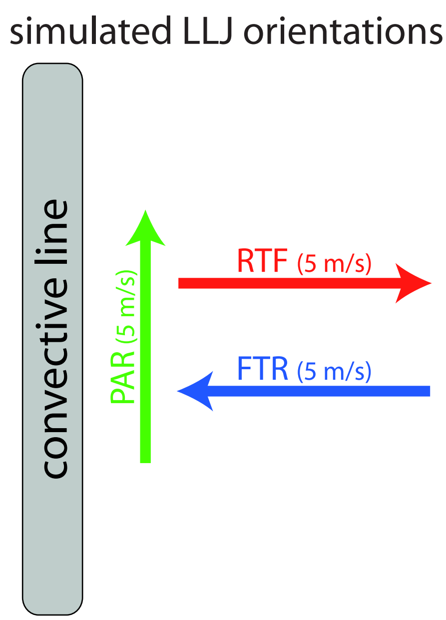

Figure 2: Schematic illustrating the different LLJ orientations used in this study.

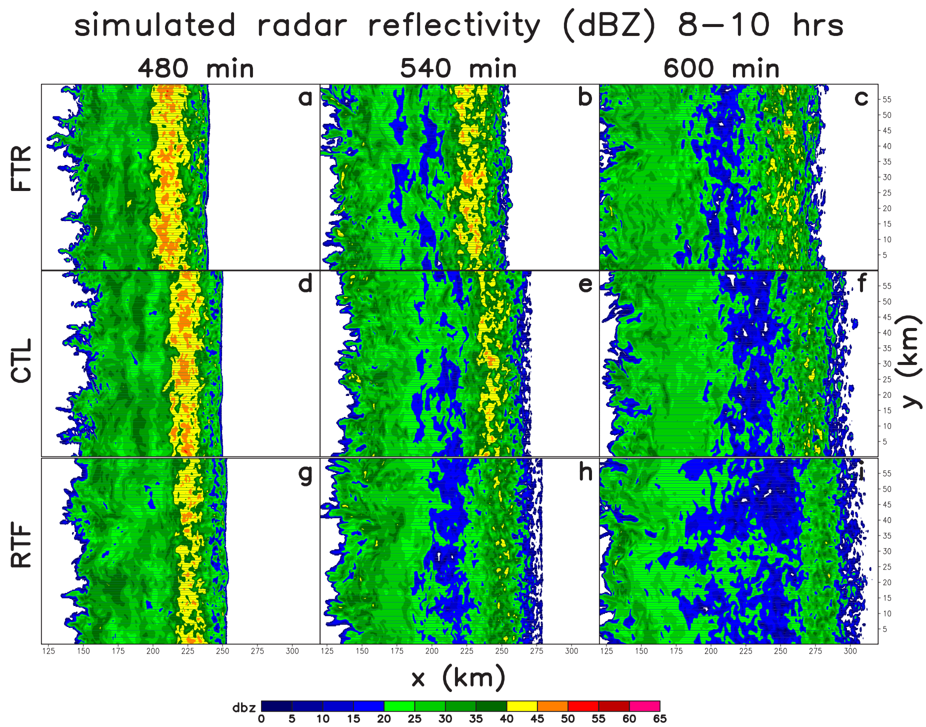

Figure 3: Plan view plots of simulated radar reflectivity (dbz) taken at z = 2 km for the CTL (a,b,c), FTR (d,e,f), and RTF (g,h,i) simulations at 480, 540, and 600 minutes into the simulation.

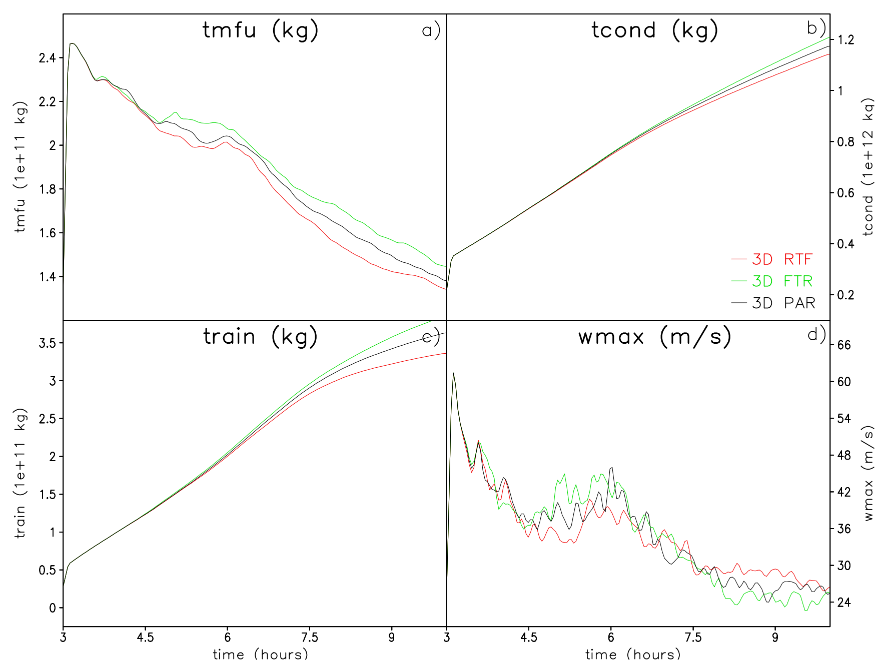

Figure 4: Time series of a) total upward mass flux (tmfu, kg), total condensate (tcond, kg), total rainfall (train, kg), and maximum vertical velocity (wmax, ms^{-1}) from 3-10 hours for the RTF (red), FTR (green) and PAR (black) simulations. The CTL and PAR simulations were very similar, so for clarity only the PAR is plotted.

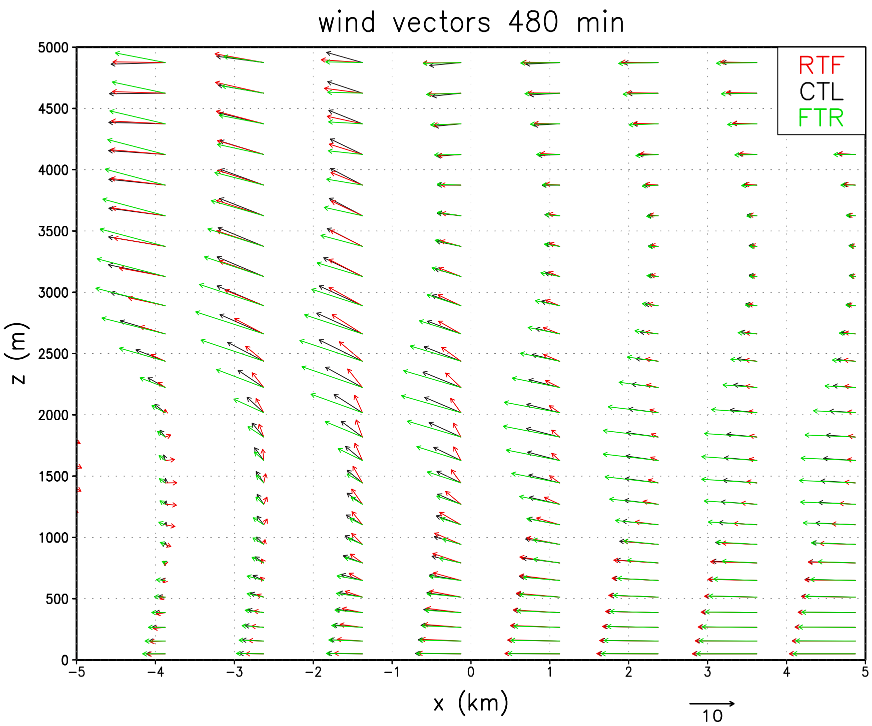

Figure 5: Cross section of along-line averaged u and w component wind vectors at 8 hours for the CTL (black), RTF (red) and FTR (green) simulations.

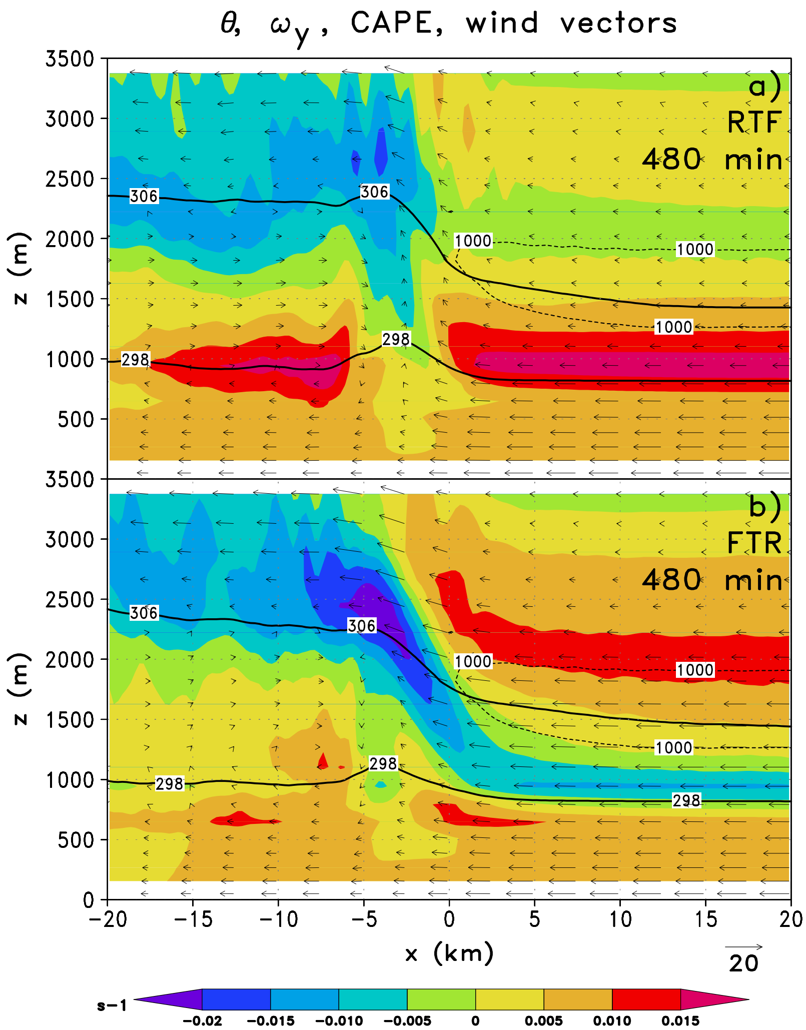

Figure 6: Vertical cross-section of along-line averaged horizontal vorticity (s^{-1}, shaded), potential temperature (K, heavy black contours), convective available potential energy (J/kg, thin, dashed contour) and storm-relative wind vectors consisting of the u and w components (ms^{-1}) for a) RTF and b) FTR simulations at 8 hours.

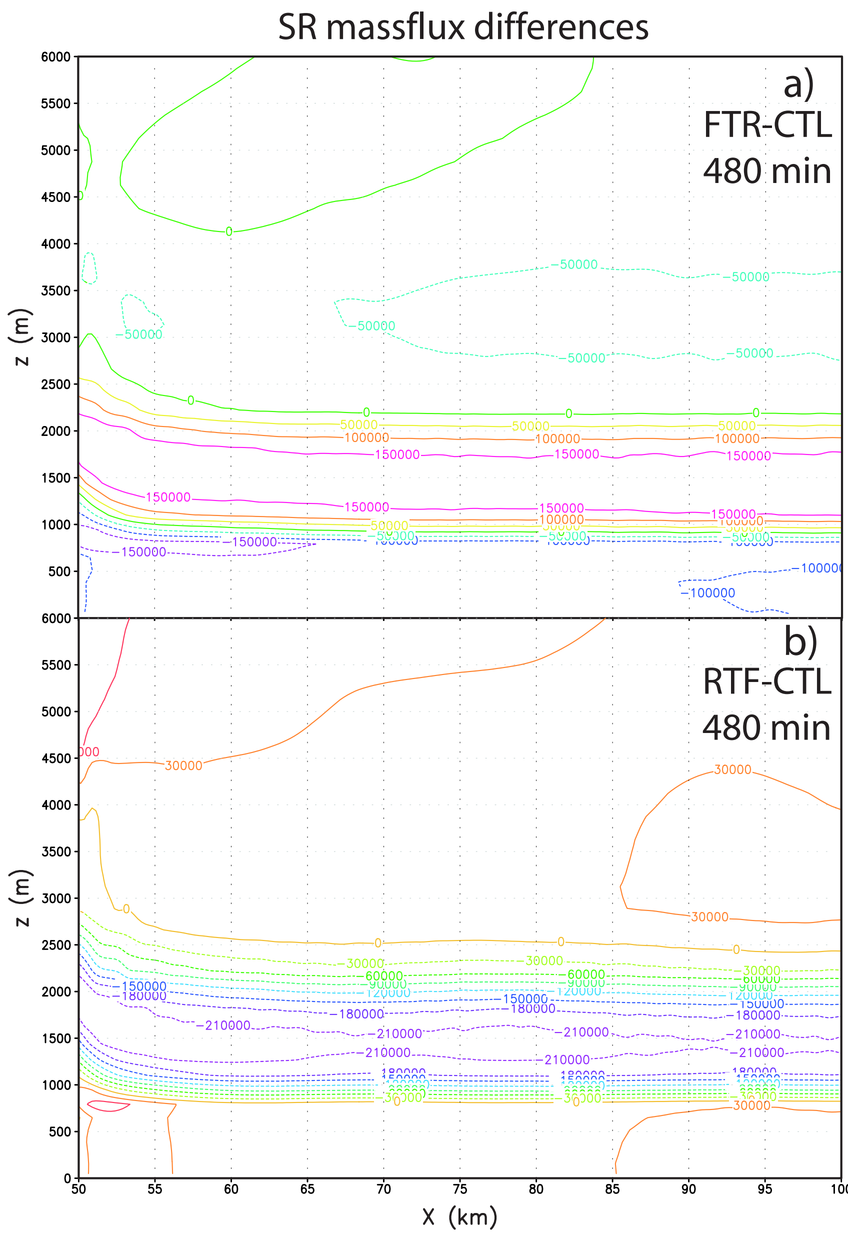

Figure 7: Vertical cross-sectional difference plots of along-line averaged storm-relative horizontal mass flux (kg/s) for a) FTR and b) RTF simulations compared to the CTL simulation.

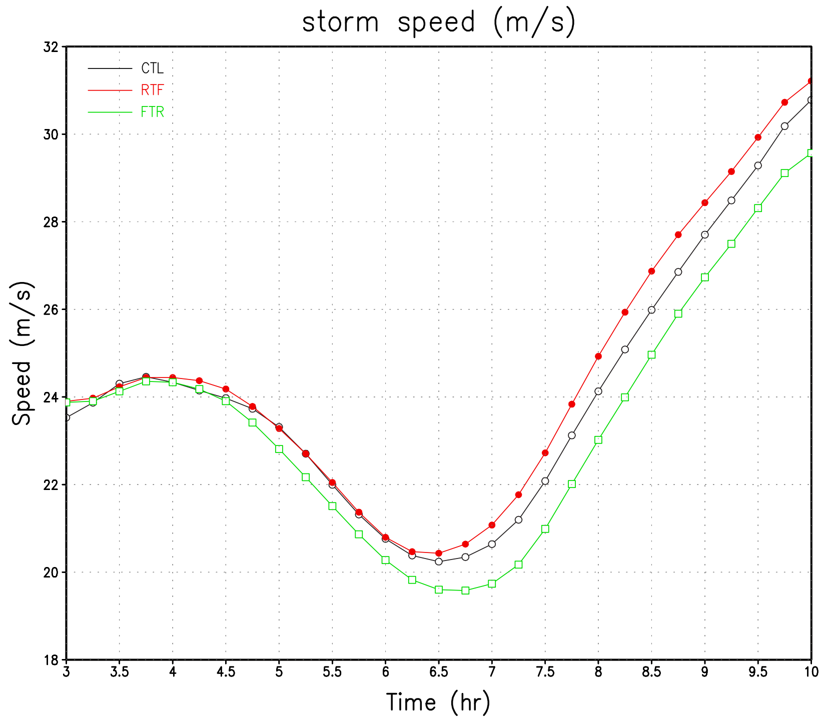

Figure 8: Time series plot of storm speed for CTL (black), RTF (red) and FTR (green) simulations.

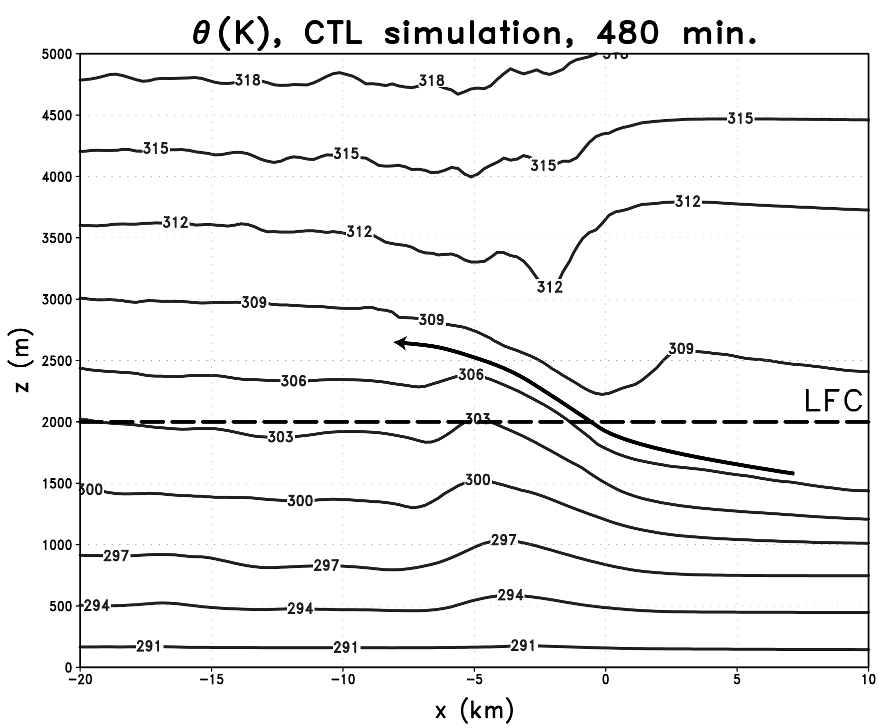

Figure 9: Cross-section of along-line averaged potential temperature at 8 hours from the CTL simulation, illustrating the depth of the bore compared to the LFC height. Dashed black line denotes the LFC height, while the curved arrow illustrates the path of parcels that cross the LFC while ascending along the bore.